Environment International 137 (2020) 105592

Contents lists available at ScienceDirect

Environment International

journal homepage: www.elsevier.com/locate/envint

Dual-modelling-based source apportionment of NO_x in five Chinese megacities: Providing the isotopic footprint from 2013 to 2014

Zheng Zong[a,b,c], Yang Tan[b,c], Xiao Wang[a], Chongguo Tian[b,c,*], Jun Li[a,*], Yunting Fang[d], Yingjun Chen[e], Song Cui[f], Gan Zhang[a]

[a] State Key Laboratory of Organic Geochemistry and Guangdong Key Laboratory of Environmental Protection and Resources Utilization, Guangzhou Institute of Geochemistry, Chinese Academy of Sciences, Guangzhou 510640, China
[b] Key Laboratory of Coastal Environmental Processes and Ecological Remediation, Yantai Institute of Coastal Zone Research, Chinese Academy of Sciences, Yantai 264003, China
[c] Center for Ocean Mega-Science, Chinese Academy of Sciences, China
[d] Key Laboratory of Forest Ecology and Management, Institute of Applied Ecology, Chinese Academy of Sciences, Shenyang 110164, China
[e] Shanghai Key Laboratory of Atmospheric Particle Pollution and Prevention (LAP3), Department of Environmental Science and Engineering, Fudan University, Shanghai 200092, China
[f] International Joint Research Center for Persistent Toxic Substances (IJRC-PTS), School of Water Conservancy and Civil Engineering, Northeast Agricultural University, Harbin 150030, China

ARTICLE INFO

Handling Editor: Hefa Cheng

Keywords:
$PM_{2.5}$
Nitrogen/oxygen isotope
NO_x source
Bayesian
PSCF
Residential coal combustion

ABSTRACT

In China, nitrate (NO_3^-) becomes the main contributor to fine particles ($PM_{2.5}$) because the emissions of its precursor, nitrogen oxides (NO_x), were not recognized and controlled well in recent years. In this work, sources, conversion, and geographical origin of NO_x were interpreted combining the isotopic information ($\delta^{15}N$ and $\delta^{18}O$) of NO_3^- and dual modelling at five Chinese megacities (Beijing, Shanghai, Guangzhou, Wuhan and Chengdu) during 2013–2014. Results showed that the $\delta^{15}N\text{-}NO_3^-$ values (n = 512) ranged from −12.3‰ to +22.9‰, and the average $\delta^{18}O\text{-}NO_3^-$ value was +83.4‰ ± 17.2‰. The isotopic compositions both had a rising tendency as ambient temperature dropped, attributing largely to the source changes. Bayesian model indicated the percentage for the ·OH pathway of NO_x conversion had a clear seasonal variation with a higher value during summer (58.0% ± 9.82%) and a lower value during winter (11.1% ± 3.99%); it was also significantly correlated with latitude ($p < 0.01$). Coal combustion was the most important source of NO_x (31.1%−41.0%), which was geographically derived from North China and other south-central developed regions implied by Potential Source Contribution Function (PSCF). Apart from Chengdu, mobile sources was the second largest contributor to NO_x. This source was extensive but uniformly distributed all around the typical urban agglomerations of China. Biomass burning and microbial processes shared similar source areas, mostly originating from the North China Plain and Sichuan Basin. Based on the NO_x features, we infer that residential coal combustion was the primary source of heavy $PM_{2.5}$ pollution in Chinese megacities. Controlling the source categories of these regional priorities would help mitigate atmospheric pollution in these areas.

1. Introduction

During the last few decades, rapid industrialization and urbanization have led to increasing occurrence of severe and persistent haze pollution in China characterized by high fine particulate matter ($PM_{2.5}$) content (Zhang and Cao, 2015). This national-scale environmental problem greatly reduces visibility and results in detrimental effects on human health. It has been observed that the number of patients with respiratory and cardiovascular diseases significantly increased during haze episodes, particularly in the most developed and highly populated city clusters (Sun et al., 2014). For addressing this extremely severe issue, the government of China has launched unprecedented campaigns to improve air quality (He et al., 2018; Xu et al., 2019). Under the umbrella of these plans, pollutant concentration levels in China are now continually decreasing (SI Fig. S1; Supporting Information, SI). The nationwide concentrations of $PM_{2.5}$, sulfur dioxide (SO_2), and nitrogen oxide (NO_x) decreased 32.8%, 43.6%,

* Corresponding authors at: Key Laboratory of Coastal Environmental Processes and Ecological Remediation, Yantai Institute of Coastal Zone Research, Chinese Academy of Sciences, Yantai 264003, China (C. Tian). State Key Laboratory of Organic Geochemistry and Guangdong Key Laboratory of Environmental Protection and Resources Utilization, Guangzhou Institute of Geochemistry, Chinese Academy of Sciences, Guangzhou 510640, China (J. Li).
E-mail addresses: cgtian@yic.ac.cn (C. Tian), lijun@gig.ac.cn (J. Li).

https://doi.org/10.1016/j.envint.2020.105592
Received 3 August 2019; Received in revised form 12 February 2020; Accepted 17 February 2020
Available online 27 February 2020

and 28.6% from 2014 to 2017, respectively. However, the decrease in NO_x in typical megacities is far less than the national average, and there has even been an increase in some instance (Si et al., 2019). For example, NO_2 concentration trends in Beijing, Shanghai, Guangzhou, Wuhan, and Chengdu during the recent four years were − 10.2%, −0.411%, +10.6%, −9.37% and − 3.07%, respectively, which were much higher the national average (−28.6%); the molar ratios of atmospheric NO_2 to (NO_2 + SO_2) increased from 0.775, 0.757, 0.793, 0.680 and 0.799 to 0.888, 0.832, 0.862, 0.873 and 0.861, respectively, in these cities; satellite observation showed an oscillation of NO_2 column concentrations in those areas; evaluation reports on $PM_{2.5}$ control effect in the Beijing-Tianjin-Hebei (BTH) city cluster since the managing campaigns revealed an increasing proportion of nitrate (NO_3^-, the resultant of NO_x) in $PM_{2.5}$ (Li et al., 2018b; Wen et al., 2018). These evidences indicate that NO_x sources are not recognized and controlled well in the Chinese urban agglomerations. In addition, NO_x is not only the precursor of NO_3^-, but it also has a crucial function in the conversion of other precursors (SI Fig. S2; Text S1) and the formation of new particles (Kharol et al., 2013). Thus, apportioning and quantifying NO_x sources are critical for the further control and improvement of air quality in Chinese megacities.

NO_x emitted from different sources has different nitrogen isotopic signals ($\delta^{15}N$). After considering the nitrogen isotopic fractionation in the transformation processes of NO_x to NO_3^-, stable N isotopes within atmospheric-derived nitrate ($\delta^{15}N$-NO_3^-) can provide an effective method to qualitatively apportion NO_x sources (Hastings et al., 2009). However, qualitative cognition is insufficient to address NO_x emissions; more reliable constraints are prerequisite (Chang et al., 2018). Bayesian models have the ability to evaluate the each contribution of different sources in a mixture, overcoming the overlaps of $\delta^{15}N$ ranges from different NO_x sources to some extent (Moore and Semmens, 2008). Based on this knowledge, we incorporated nitrogen fractionation of the equilibrium/Leighton reaction during conversion from NO_x to NO_3^- into a Bayesian model (the stable isotopic mixing model using sampling-importance-resampling [MixSIR]), and adopted the improved model to apportion annual NO_x sources in North China (Zong et al., 2017). In addition to apportioning NO_x sources, this model is also capable of assessing conversion pathways for NO_x (SI Text S2; SR_4: the ·OH pathway, SR_5-SR_7: the O_3 pathway), which, of course, provides effective information for NO_x governance (Madaniyazi et al., 2016).

Previous research studies focusing on the Chinese air quality have involved most particulate constituents, such as organic carbon (OC), black carbon (BC), ammonium (NH_4^+), sulfate (SO_4^{2-}), and their precursors (e.g., volatile organic compounds [VOCs], ammonia [NH_3], SO_2) (Ding et al., 2016; Liu et al., 2014; Pan et al., 2016; Sun et al., 2014; Wu and Xie, 2018; Zhang et al., 2014), while NO_3^- or NO_x sources remain poorly constrained. Moreover, the current NO_x researches using $\delta^{15}N$ analysis are mainly aimed at a single city or limited region, which may lack linkage and comparative information between cities under the same analytical system. Therefore, multi-city simultaneous study, providing more scientific theory for NO_x governance, will be an inevitable trend to further apportion urban NO_x in China. According to the present situation and problems of NO_x, multi-city $PM_{2.5}$ sampling including Beijing, Shanghai, Wuhan, Chengdu, and Guangzhou was conducted from 2013 to 2014 in this research. These cities comprise BTH, Yangtze River Delta (YRD), middle reaches of the Yangtze River (MYR), Sichuan-Chongqing (SC), and Pearl River Delta (PRD) city clusters, respectively. Satellite remote sensing indicates these selected areas are the most polluted areas in terms of NO_x in China (SI Fig. S3).

The objectives of this study are to (1) detect the multi-city $\delta^{15}N$ and stable oxygen isotope ($\delta^{18}O$) characteristics of NO_3^- in $PM_{2.5}$, (2) quantitatively estimate NO_x sources and its conversion pathways using the improved Bayesian model, (3) explore the geographical origin of NO_x utilizing the Potential Source Contribution Function (PSCF), and (4) reveal the source factor leading to the heave $PM_{2.5}$ pollution in Chinese megacities. In terms of innovation, this study interprets the isotopic information of NO_x from a multi-city scale in China, and reveals the significant correlation between ·OH pathway of NO_x conversion and latitude from the aspect of $\delta^{18}O$.

2. Materials and methods

2.1. Sampling and weighing

The sampling was conducted from October 2013 to August 2014 at five Chinese megacities (Beijing: 116.34 °E, 39.93 °N; Shanghai: 121.50 °E, 31.29 °N; Wuhan: 104.36 °E, 30.52 °N; Chengdu: 104.38 °E, 30.64 °N; Guangzhou: 113.36 °E, 23.15 °N). Detailed reasons to select these cities can be referred in SI Text S3. One month was selected every season for sampling every day; the duration for each sample was 24 h, and finally 512 $PM_{2.5}$ samples were obtained. Details regarding the sampling are summarized in SI Table S1 (Liu et al., 2017a). Noted, significant test of the NO_x concentrations in our sampling period and its season shows that all p-values in each of the five cities are greater than 0.05 (SI Table S2). This indicates that there is no significant difference in NO_x concentrations between our sampling period and its season, and the pollution characteristic of our sampling period can represent the corresponding season (Hollaway et al., 2019; Zhao et al., 2013). Fine particles were collected on quartz fiber filters (preheated for 5 h at 450 °C) by high-volume samplers (Andersen Instruments/GMW) operated at 0.3 m^3 min^{-1} (calibrated every three days). Then the filters were stored at − 20 °C in a refrigerator until analysis. Before and after each sampling, the filters would pass through an equilibration of 25 °C and 39% relative humidity (RH) for 24 h, which was followed by the weigh based on an MC5 electronic microbalance (± 10-μg) for calculating the $PM_{2.5}$ concentration. Each weighing was repeated three times with the difference: ≤ 10 μg for the blank filters; ≤ 20 μg for the sampled filters (Liu et al., 2016).

2.2. Isotopic and chemical analysis

The nitrous oxide (N_2O) isotopic analysis method was used to quantify $\delta^{15}N$-NO_3^- and $\delta^{18}O$-NO_3^- at the five cities (n = 512) (McIlvin and Altabet, 2005). Briefly, NO_3^- solution was diluted to 15 μmol L^{-1}, and the total volume and NaCl concentration should be limited to 5 mL and 0.5 mol L^{-1}, respectively. Then Cd in powder form (0.3 g) was added with the injection of imidazole solution (1 mol L^{-1}, 0.1 mL) to adjust the pH to 9. After tightly capped, the processed samples were ultrasonically oscillated (40 °C for 2 h). In the process, NO_3^- was reduced to nitrite (NO_2^-) with a conversion rate of 98.0% ± 7.89%. The reaction solution was allowed to stand for 12 h and then 4 mL was taken to a new bottle, where sodium azide (20% acetic acid and sodium azide mixed in a 1:1 vol ratio, and purified with helium for 60 min) was injected at the same time. After 30 min, 0.4 mL of 10 mol L^{-1} NaOH was added to terminate the reaction. The N_2O produced by the reaction was used to detect $\delta^{15}N$ and $\delta^{18}O$ on an isotope ratio mass spectrometer (MAT253) and the values were expressed in parts per thousand, taking international reference materials (IAEA-NO_3^-, USGS32, USGS34, and USGS35) as the standards:

$$\delta^{15}N = [(^{15}N/^{14}N)_{sample}/(^{15}N/^{14}N)_{standard} - 1] \times 1000 \quad (1)$$

$$\delta^{18}O = [(^{18}O/^{16}O)_{sample}/(^{18}O/^{16}O)_{standard} - 1] \times 1000 \quad (2)$$

The analytical precision was less than 0.36‰ for $\delta^{15}N$ and 0.52‰ for $\delta^{18}O$, respectively, determined from the replicates. Since the concentrations of NO_2^- were below the detection limit and less than 0.31% of NO_3^-, this part was not considered in the isotopic analysis (Wankel et al., 2006). Routine chemical methods (SI Text S4) was used to measure the concentrations of OC, EC and major ions including K^+, Ca^{2+}, Na^+, Mg^{2+}, Cl^-, NO_3^- and SO_4^{2-} (Zong et al., 2016).

2.3. Bayesian model

With isotopic features, Bayesian model could identify the probability distribution of the contribution of each source to a mixture, and clearly explain for the uncertainty, which is related with multiple sources, fractionation, and isotopic signatures (Parnell et al., 2013). Therefore, the model has been diffusely employed in ecological study (e.g., food-web research) (Moore and Semmens, 2008). Nonetheless, challenges remain in applying the model to atmospheric research because of the difficulty of quantifying isotopic fractionation during atmospheric processes. In our previous research, the Bayesian model (MixSIR) was improved by incorporating the isotopic fractionation of the equilibrium/Leighton reaction (Zong et al., 2017). Briefly, the difference between δ^{15}N-NO_3^- in the atmosphere and δ^{15}N-NO_x emitted from sources can be considered as a hybrid contribution through two dominant isotopic exchange reaction processes as follows (Walters and Michalski, 2016):

$$\begin{aligned}\Delta N &= \gamma \times \Delta(\delta^{15}N - NO_3^-)_{OH} + (1-\gamma) \times \Delta(\delta^{15}N - NO_3^-)_{H_2O} \\ &= \gamma \times \Delta(\delta^{15}N - HNO_3)_{OH} + (1-\gamma) \times \Delta(\delta^{15}N - HNO_3)_{H_2O}\end{aligned} \quad (3)$$

where $\Delta(\delta^{15}\text{N-NO}_3^-)_{OH}$ is the isotopic difference caused by the reaction between NO_2 and photochemically produced ·OH, and γ is its contribution ratio. Similarly, $\Delta(\delta^{15}\text{N-NO}_3^-)_{H2O}$ is the isotopic difference resulting from the hydrolysis of N_2O_5 forming on a wetted surface. It is assumed that no kinetic isotopic fractionation occurs in the reaction of NO_2 and ·OH, the $\Delta(\delta^{15}\text{N-HNO}_3)_{OH}$ and $\Delta(\delta^{15}\text{N-HNO}_3)_{H2O}$ can be calculated using mass-balance, respectively, as follows:

$$\begin{aligned}\Delta(\delta^{15}\text{N - HNO}_3)_{OH} &= \Delta(\delta^{15}\text{N - NO}_2)_{OH} \\ &= 1000 \times \left[\frac{(^{15}\alpha_{NO_2/NO}-1)(1-f_{NO_2})}{(1-f_{NO_2})+(^{15}\alpha_{NO_2/NO}\times f_{NO_2})}\right]\end{aligned} \quad (4)$$

$$\begin{aligned}\Delta(\delta^{15}\text{N - HNO}_3)_{H_2O} &= \Delta(\delta^{15}\text{N - N}_2\text{O}_5)_{H_2O} \\ &= 1000 \times (^{15}\alpha_{N_2O_5/NO_2}-1)\end{aligned} \quad (5)$$

where $^{15}\alpha_{NO2/NO}$ refers to the equilibrium isotopic fractionation factor between NO_2 and NO, and $^{15}\alpha_{N2O5/NO2}$ is corresponding value between N_2O_5 and NO_2; they are all temperature-dependent functions (SI Table S3). f_{NO2} is the proportion of NO_2 in the total NO_x, typically ranging from 0.2 to 0.95. In addition, γ could be calculated by the fractionation information of δ^{18}O-NO_3^- using the analogical principle and process. For the particular model framework and computing method, readers can refer to our previous research (Zong et al., 2017). In this work, coal combustion (+13.7‰ ± 4.57‰), mobile sources (−7.24‰ ± 7.77‰), biomass burning (+1.04‰ ± 4.13‰), and microbial processes (−35.4‰ ± 10.7‰) were confirmed as the major contributors to NO_x at the five megacities (SI Text S5; Table S4). Bayesian model was operated for three scenarios (overall, seasonal and heavy $PM_{2.5}$ pollution simulations) to show the comprehensive source information of NO_x.

2.4. PSCF model

PSCF is a conditional probability describing the spatial distribution of probable geographical source locations inferred by using trajectories (HYSPLIT model, SI Text S6) arriving at the sampling site (Bressi et al., 2014). In this study, the model was adopted to evaluate the potential NO_x source regions of the indicative source factor from the Bayesian model using the respective resulting data. Generally, the ij_{th} component of a PSCF field can be written as follows:

$$PSCF_{ij} = m_{ij}/n_{ij} \quad (6)$$

where n_{ij} is the total number of end points dropped in the ij_{th} cell, and m_{ij} is the number of endpoints of the package whose measured value exceeds the threshold criteria determined by the user. For improved accuracy, we integrated the $PSCF_{ij}$ of the five cities together in the model (Specific simulation program can be referred in SI Fig. S5). Notably, cells with few endpoints can lead to high uncertainty. Therefore, to eliminate these high uncertainties, an arbitrary weight function $W(n_{ij})$ is multiplied into the PSCF value as follows (Jeong et al., 2011):

$$W(n_{ij}) = \begin{cases} 1.00\ (n \geqslant 40) \\ 0.70\ (10 \leqslant n \leqslant 40) \\ 0.42\ (5 \leqslant n \leqslant 10) \\ 0.17\ (n \leqslant 5) \end{cases} \quad (7)$$

In the present study, we performed two PSCF scenarios. The first scenario showed the contribution level of regions in terms of NO_x using the resulting data with the 75th percentile cut of each source factor from the Bayesian model (Xie et al., 2015), and the second exposed the source region of the highest 25% of the $PM_{2.5}$ concentrations in the five cities.

2.5. $PM_{2.5}$ concentration partition

High $PM_{2.5}$ concentration and its sources have always been the focuses of attention in pollution control of particulate matter. In this study, their connections with NO_x emission were explored. For a better description, we artificially divided the heavy pollution stage (HP stage) and the non-heavy pollution stage (NHP stage) according to the concentration of $PM_{2.5}$. Generally, concentration classification would be the most scientific according to the national (e.g. In China, the annual and 24-hour average $PM_{2.5}$ concentration limits are set at 35 μg m^{-3} and 75 μg m^{-3}, respectively) or world (e.g. For WHO, the annual and 24-hour average $PM_{2.5}$ concentration limits are set at 10 μg m^{-3} and 25 μg m^{-3}, respectively) standards. However, the sampling period was from 2013 to 2014, when $PM_{2.5}$ pollution was raging in the targeted Chinese megacities. Correspondingly, $PM_{2.5}$ concentrations were much higher than those stated standards. For example, the observed average $PM_{2.5}$ concentration in Beijing was 186 ± 92.2 μg m^{-3} (Section 3.1). Therefore, it is not suitable to use the standards to divide pollution days in this study. Based on the principle of published articles (Xie et al., 2015;Xu et al., 2018), this article uses a 75% higher and 25% lower method to distinguish between HP stage and NHP stage weather, respectively. Therein, the threshold values of 25% and 75% belong to the high and low value intercept points in the statistical quartile, which may better reflect the characteristics of heavy pollution stage in each city.

3. Results and discussion

3.1. Concentration features of $PM_{2.5}$ and NO_3^-

The annual $PM_{2.5}$ concentrations at Beijing, Shanghai, Wuhan, Chengdu, and Guangzhou were 186 ± 92.2 μg m^{-3}, 87.7 ± 48.5 μg m^{-3}, 137 ± 56.4 μg m^{-3}, 159 ± 66.9 μg m^{-3}, and 77.7 ± 28.1 μg m^{-3}, respectively. All exceeded the Second Grade National Standard of China (75 μg m^{-3}), indicating poor air quality nationwide from 2013 to 2014. Geographically, the particulate pollution was more serious in Beijing, Wuhan, and Chengdu compared to that in Shanghai and Guangzhou, which may be partly because of their locations. Shanghai and Guangzhou are proximal to the ocean (SI Fig. S3), where relatively clean air can alleviate the severe $PM_{2.5}$ pollution. NO_3^- is a substantial component in $PM_{2.5}$, and was 25.8 ± 26.8 μg m^{-3}, 15.6 ± 15.8 μg m^{-3}, 9.13 ± 10.2 μg m^{-3}, 15.3 ± 14.4 μg m^{-3}, and 16.4 ± 12.4 μg m^{-3} in Beijing, Shanghai, Guangzhou, Wuhan, and Chengdu, respectively. As previously mentioned, NO_3^- forms from the conversion of NO_x; thus, $PM_{2.5}$ may possess the same secondary traits (r greater than 0.69 between $PM_{2.5}$ and NO_3^-; $p < 0.01$). Combining with SO_4^{2-}, NH_4^+, and secondary organic carbon (SOC) (SI Text S7), secondary components were identified as the most important contribution to $PM_{2.5}$, with a ratio of 52.1% in Guangzhou, 48.9% in Shanghai, 44.8% in Wuhan, 37.2% in Beijing, and 35.0% in Chengdu, respectively (SI Fig. S6).

Despite the large variation within the five cities, $PM_{2.5}$ concentrations were always higher during winter (average: 178 ± 25.1 μg m^{-3}),

showing an obvious seasonal fluctuation (SI Fig. S7). Similarly, NO_3^- shared a parallel seasonal variation with $PM_{2.5}$ showing a higher concentration during winter (27.2 ± 15.7 μg m^{-3}) and lower during summer (6.76 ± 6.44 μg m^{-3}) at the five cities. Atmospheric pollutant concentrations are generally governed by emissions and meteorological conditions (Tao et al., 2014). Therefore, the higher concentrations in cool season can be ascribed in part to the relatively weaker atmospheric horizontal diffusion ability and vertical exchange capacity (Guo et al., 2014). Furthermore, residential coal combustion in wintertime is also an important additional emission source at that time (Chen et al., 2017). Certifiably, $PM_{2.5}$ concentration and NO_3^- concentration both had a certain negative correlation with the wind speed and temperature during the sampling period (SI Fig. S8; Table S5).

3.2. Source and conversion of NO_x based on N and O isotopic signals

δ^{15}N-NO_3^- values in the five cities ranged from − 12.3‰ to + 22.9‰ (Wuhan: +6.38‰ ± 6.09‰; Beijing: +5.46‰ ± 7.67‰; Shanghai: +3.33‰ ± 4.63‰; Guangzhou: +2.32‰ ± 5.99‰; Chengdu: +0.79‰ ± 5.04‰) (SI Fig. S9) along with significant seasonal variation. Higher values typically appeared during winter, followed by autumn or spring, and lower values occurred during summer (Fig. 1). The situation of Chengdu was not very consistent, which was ascribed to its air flow being obviously different from that of the other cites (SI Fig. S10). Beijing, Shanghai, Wuhan, and Guangzhou all have a definitive monsoonal climate, with prevailing approximately southerly winds during summer and northerly winds during winter (Yihui and Chan, 2005). It results in regional pollutants to be efficiently transported and mixed across the four sites, presenting a similar δ^{15}N-NO_3^- tendency. While the airflow in Chengdu is relatively stable with a prevalence of easterly winds and westerly winds during the year, resulting in distinctive δ^{15}N-NO_3^- information.

In the atmosphere, NO_3^- largely derives from the conversion of NO_x, whose δ^{15}N-NO_x values have been reported to be widely dispersed from different sources (Felix and Elliott, 2014; Felix et al., 2012; Walters et al., 2015). According to the fractionation theory in the conversion of NO_x to NO_3^-, a low temperature during the cold season may result in more obvious nitrogen isotopic fractionation than during the warm season (Walters and Michalski, 2015). To assess the impact of temperature on the δ^{15}N-NO_3^- value, we calculated the nitrogen isotopic fractionation between summer and winter with the highest and lowest temperatures, respectively. We found that nitrogen isotopic fractionation induced by temperature between summer and winter was approximately 3.48‰, 2.57‰, 3.16‰, 2.80‰ and 0.812‰ in Beijing, Shanghai, Wuhan, Chengdu, and Guangzhou, respectively, much lower than the real nitrogen isotopic difference between the two seasons of 7.36‰, 8.54‰, 9.96‰, 7.72‰ and 10.4‰. Thus, the low values during summer and high values during winter can be attributed to more microbial processes and coal combustion, respectively, according to the source value distribution (Elliott et al., 2019). In China, coal combustion can be generally divided into two main categories: industrial coal (e.g., a power plant) and residential coal (e.g., for heating combustion). Because the emission intensity of the former is relatively stable throughout the year, the higher δ^{15}N-NO_3^- during winter was inferred to have been derived from the additional civil use for domestic heating in North China. This was verified by the highest δ^{15}N-NO_3^- (+13.8‰ ± 5.02‰) during winter in Beijing, as only one of the five cities requires civil heating during winter. The δ^{15}N-NO_3^- value in Wuhan was comparable to that in Beijing during winter, because the air masses arriving at Wuhan mostly pass through the heating area (SI Fig. S10), while lower values were correspondingly found in the indirect air flow of the other sites, including Shanghai, Guangzhou, and Chengdu.

In the NO/NO_2 cycle (SI SR_1–SR_3), the oxygen atoms of atmospheric NO_x are rapidly exchanged with O_3, then NO_2 is converted to HNO_3 based on ·OH or O_3 (SI SR_4–SR_7). Thus, the δ^{18}O-NO_3^- value is controlled by the generation pathways, which could be utilized to estimate the conversion processes of NO_x to NO_3^- (Morin et al., 2009). The average δ^{18}O-NO_3^- observed (SI Fig. S11) revealed a decreasing trend from north to south: Beijing (+89.0‰ ± 15.0‰), Shanghai (+85.4‰ ± 17.9‰), Wuhan (+81.0‰ ± 15.0‰), Chengdu (+84.9‰ ± 18.0‰), and Guangzhou (+76.7‰ ± 17.9‰), well within the broad range of values presented in previous reports (Elliott et al., 2009;Morin et al., 2008). In the Bayesian modelling framework, it is assumed that the oxygen atoms of NO_3^- derive from 2/3 O_3 and 1/3 ·OH in the ·OH pathway (SI SR_4), and from 5/6 O_3 and 1/6 ·OH in the O_3 pathway (SI SR_5-SR_7). Based on the reported values for δ^{18}O-O_3 and δ^{18}O-H_2O (Fang et al., 2011;Vicars et al., 2012), the contributions of the two generation pathways were assessed using a Monte Carlo simulation. The result (median ± standard deviation) of the proportion for the ·OH pathway is demonstrated in Fig. 2. Annually, the median ranged from 23.6% to 39.6%, well within the global model prediction results (Alexander et al., 2009). The median had a clear seasonal variation at all sites with a higher value during summer (58.0% ± 9.82%) and lower value during winter (11.1% ± 3.99%).

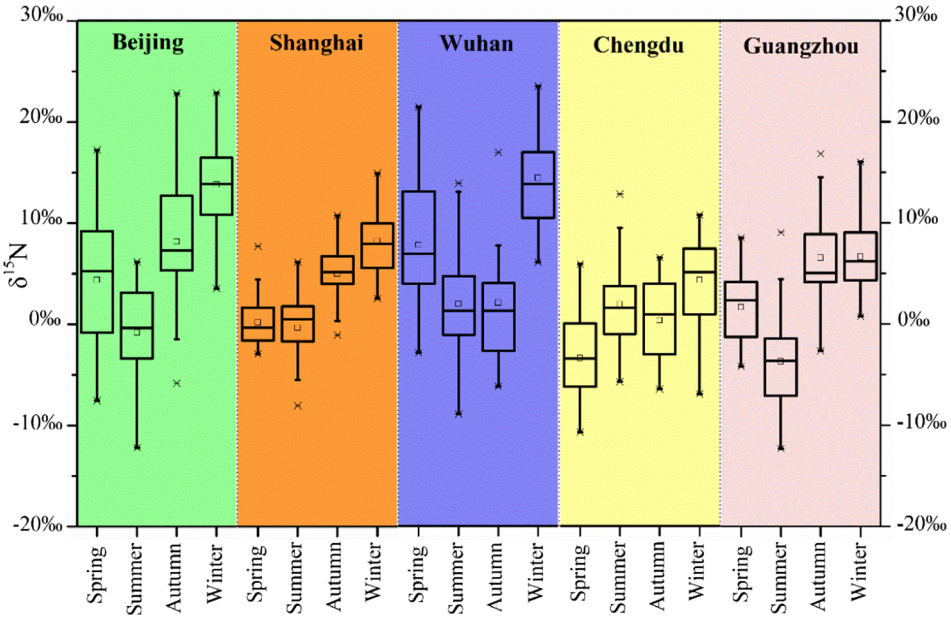

Fig. 1. Seasonal characteristic of δ^{15}N-NO_3^- in Beijing, Shanghai, Wuhan, Chengdu, and Guangzhou during the 2013–2014 period.

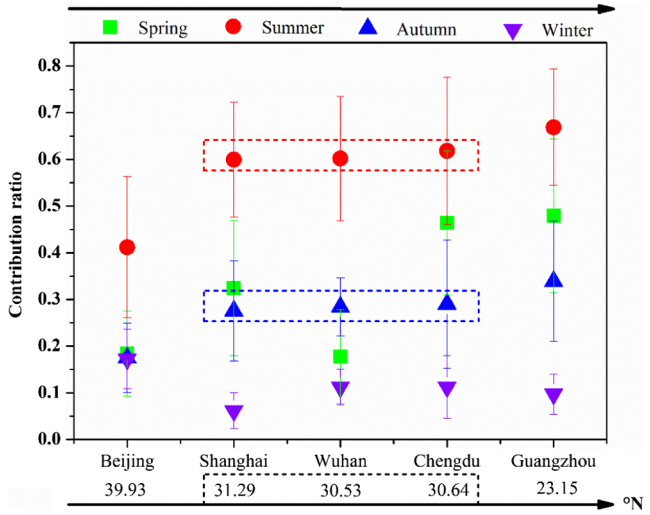

Fig. 2. The characteristic of the contribution ratio of the ·OH conversion pathway for NO_x at the five cities indicated by the Bayesian model.

This suggested the ·OH generation pathway during summer and the O_3 generation pathway in winter were the main pathways for NO_x conversion, respectively. This result was in accordance with the mean value of $\delta^{18}O\text{-}NO_3^-$ being +68.4‰ ± 14.2‰ during summer and +99.7‰ ± 11.5‰ during winter for the five cities. Interestingly, Shanghai, Wuhan, and Chengdu are approximately at the same latitude, and their median was basically consistent (in summer and autumn) and lower than that of Guangzhou and higher than that of Beijing. Using the linear mixed effect model by R Language (SI Text S8), we further found that the proportion of the ·OH pathway for NO_x conversion shares a significant ($p < 0.01$) correlation with latitude all year-round. Generally, the formation of ·OH is affected by many factors, such as the O_3 concentration, air humidity and UV radiation intensity. Among these factors, latitude could be a proxy for UV as previous studies have shown that they share a certain global correlation with each other (SI Fig. S12). Although there is no specific UV data, we inferred that UV radiation intensity may be the most important factor for ·OH generation pathway of NO_x based on its significant correlation with latitude found here. The finding provides favorable evidence for previous modelling predictions (Alexander et al., 2009;Spivakovsky et al., 2000). It is the first time revealing the correlation between ·OH pathway of NO_x conversion and latitude from the aspect of $\delta^{18}O$.

3.3. Source apportionment of NO_x using Bayesian model

The overall estimation showed that coal combustion was the most important source for NO_x with a contribution of 40.4% ± 12.3%, 34.0% ± 8.28%, 41.0% ± 13.7%, 31.1% ± 4.89%, and 33.8% ± 10.2% in Beijing, Shanghai, Wuhan, Chengdu, and Guangzhou, respectively (Fig. 3). This finding was in agreement with the characteristics of energy consumption in China (SI Fig. S13). Coal combustion is dominant in the energy combustion, but the proportion is gradually decreasing. Under the "Twelfth Five-Year Plan for National Environment Protection" in China, NO_x emissions from coal-fired power plants has decreased, mainly because of the widespread installation of pollution control equipment. As reported, 95% of power plants in China had installed NO_x removal systems by 2015; NO_x from power plants decreased 45% during the period of 2010–2015 (Tong et al., 2010). Coal combustion has a distinct seasonal fluctuation with a higher contribution during winter (Beijing: 58.7% ± 17.6%; Shanghai: 42.6% ± 12.1%; Wuhan: 54.5% ± 12.8%; Chengdu: 34.3% ± 5.33%; Guangzhou: 38.9% ± 12.6%) when great amounts of coal are consumed for residential heating in northern China (Cai et al., 2018), which also accords with the variation in $\delta^{15}N$ previously discussed. This suggested residential coal combustion could not be ignored during the treatment of NO_x pollution. Illustratively, the lowest contribution occurred in Chengdu, in which the air masses do not pass through the heating area (SI Fig. S10). In addition, our finding is also consistent with previous results on Beijing. Song et al., 2019 reported that coal combustion was the dominant contribution (28 ± 13%) for NO_x along with obvious seasonal variation in 2014 (Song et al., 2019); Luo et al., 2019 revealed that the fractional contribution of coal

Fig. 3. Contributions of biomass burning, coal combustion, mobile sources, and microbial processes to NO_x at the five sites and their seasonal variation.

combustion to NO_x during late winter through spring could reach to 54.4 ± 8.4% in 2013 (Luo et al., 2019). Although there is some difference in those analytical results due to the end members of source values and isotopic fractionation adopted in the Bayesian model, the seasonal consistency confirms the authenticity of our results.

Apart from Chengdu, mobile sources was the second largest contributor to NO_x. The rapid growth of automobile ownership makes vehicle exhaust become an important source for NO_x pollution. According to the car industry surveys, car ownership in China has grown by 14.0% a year since 2009. Moreover, environmental air quality, especially in coastal areas, is severely affected by ship emissions. It was estimated that 11.3% of the total NO_x emissions in 2013 came from ships (Zhang et al., 2016). Therefore, the observed increase in the contribution of mobile sources can also be ascribed to ship emissions. This contribution has not significantly changed throughout the year, agreeing with the emission intensity because vehicles or ships are running all year round (Li et al., 2018a).

Large-scale biomass burning and the prevalence of household emissions have significantly increased NO_x emissions. From 1990 to 2013, the NO_x emissions induced by biomass burning increased more than six-fold in China (Li et al., 2016). At Chengdu, biomass burning contributed the most among the five cities, up to 26.8% ± 2.67%. Such a high contribution was consistent with the contribution to EC based on ^{14}C measurement (Liu et al., 2017a). There is no significant seasonal change indicating biomass fuel is used during an entire year as a conventional fuel around Chengdu. A similar situation emerged at Shanghai and Guangzhou. However, the source peaks during autumn and summer at inland Beijing and Wuhan influenced by the large-scale biomass burning surrounding the regions (Wang et al., 2014). China is an agriculture-oriented country with a large area of cultivated land (SI Fig. S14). Microbial bacteria widely distributed in soils consume accumulated nitrogen (NH_4^+ by nitrifying microbes, NO_3^- by denitrifying microbes) and as a by-product, to the release of large pulses of NO (Jaeglé et al., 2004). Thus, extensive cultivated land where nitrogen fertilizer overused is an important source of NO_x in China. In addition, marine sediments and estuaries are also part of denitrification areas (Wankel et al., 2006). Although the contribution of marine bacteria to NO_x has not been widely reported, the ocean surrounding China may also contribute to NO_x based on the similar activity mechanism of bacteria, particularly during summer when the synoptic system is dominated by the southeast monsoon from the sea. The contribution of integrated microbial processes ranged from 14.0% to 19.1% among the five cities. It shows an obvious seasonal variation with a typically high value during summer, consistent with the state of the environment (hot and rainy weather) at the time (Yihui and Chan, 2005). The highest contribution was found at Chengdu, controlled by the nearby large area of cultivated land. This indicated that soil microbial process was more important than marine ones. The lowest occurred at Beijing, mainly due to the state of its natural environment (e.g. lower temperature and precipitation in cool season). Because in the rainy and hot summer season, its contribution (20.8 ± 3.95%) was basically the same as that of other cities (Shanghai: 20.6 ± 2.45%; Wuhan: 19.9 ± 4.67%; Chengdu: 18.4 ± 4.27%; Guangzhou: 22.4 ± 3.63%).

3.4. Spatial sources of NO_x deduced from PSCF analysis

Fig. 4 reports the PSCF map produced using the resultant data with the 75th percentile cut of each source factor from the Bayesian model. Obviously, the region surrounding the North China Plain and Sichuan Basin were identified as the medium to high potential regions for biomass burning, consistent with the distribution of cultivated land in China (SI Fig. S14) (Ning et al., 2018). In farming areas, agricultural wastes are often stored as fuel for home cooking or heating, while other

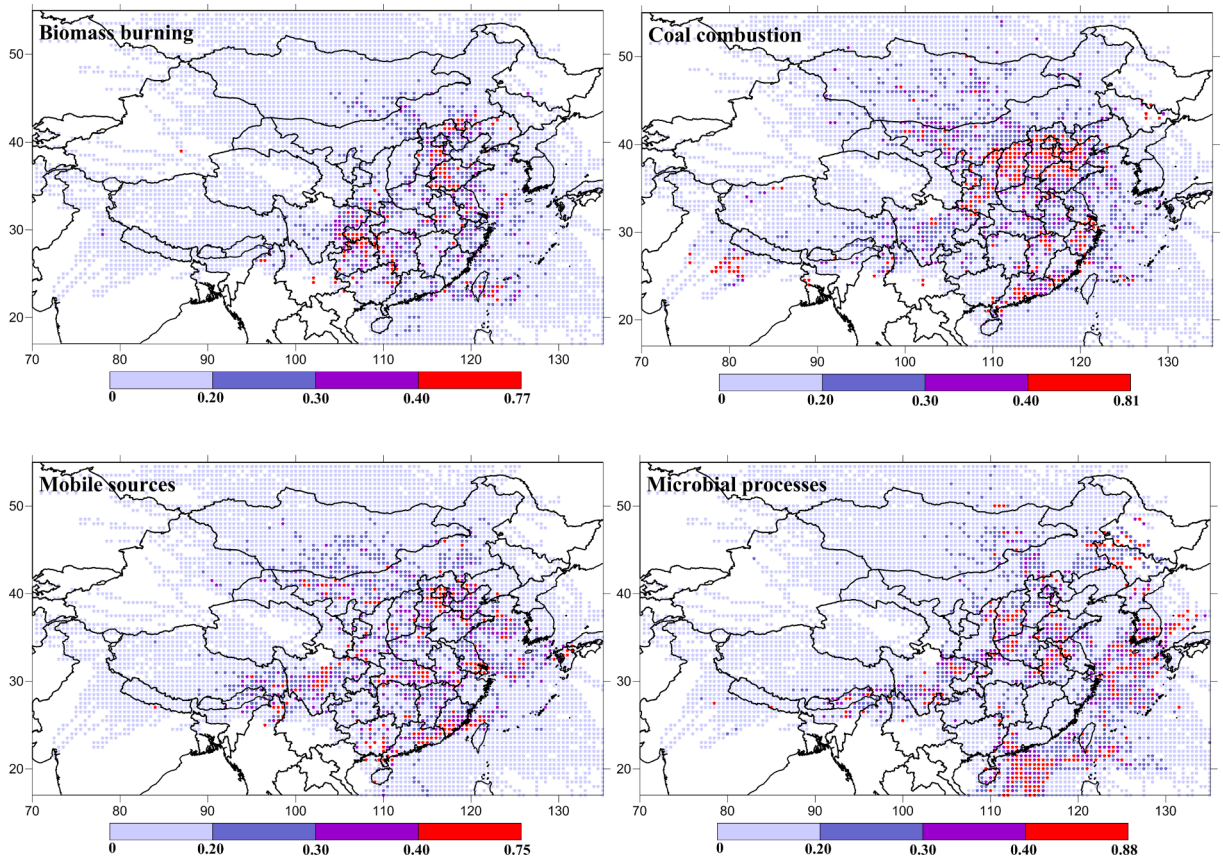

Fig. 4. PSCF maps of the contributions of biomass burning, coal combustion, mobile sources, and microbial processes to NO_x from October 2013 to August 2014. The colors represent the contribution level of the regions; the dark color has a high probability of becoming a source region, while the light color indicates a low possibility.

wastes are consumed rapidly through open burning in fields. Thus, farming area is an important source region for biomass-burning NO_x. For example, our previous study suggested biomass burning from Shandong, Anhui, and Jiangsu province (around the North China Plain) contributed a large portion of $PM_{2.5}$ (Zong et al., 2015). Shandong and Sichuan area were found to have the highest biomass burning contribution to NO_x in this study, agreeing with the regional distribution of the high-resolution emission inventory of open biomass burning in China (Qiu et al., 2016). Notably, NO_x was emitted more west and south of Shandong province (Gao et al., 2017).

For coal combustion, there are a large number of grid cells with PSCF values greater than 0.4 in North China and other south-central developed regions. The vast stretch of source area in North China can be partly attributed to the huge power plant emission in China's coal-producing areas, such as Shanxi and Shandong province. According to the China Statistical Yearbook, the coal production in Shanxi and Shandong province ranks second and sixth, respectively, in China, and their thermal power generation both exceeds 250 TWh (Yearbook, 2014). However, additional civil heating coal consumption during winter makes the contribution in the region more apparent. In China, residential consumption of coal has been calculated to be approximately 7 billion tons per year (Yearbook, 2015). Based on the emission calculation, the pollution load from these households without pollution control devices would be equal to the pollution load from 460 billion tons of coal-fired power plants. Such huge emissions may be among the factors affecting the intensification of pollution during winter. Previous study also showed coal combustion in residential stoves was a widespread source from urban to rural areas in North China on the basis of many analytical tools (Chen et al., 2017). In addition, the regional diffusion may cause the Bohai Sea to become a secondary source region. Other south source areas were in accordance with thermal power generation at the province level, such as the high possibility in Jiangsu, Zhejiang, Guangdong etc (SI Fig. S15) (Ming et al., 2016), proving that the combustion of coal in these areas basically originates from power plant emission.

Compared to other sources, mobile sources are more extensive, but rather uniformly distributed all around the typical urban agglomerations in China, such as the BTH city groups, the YRD city groups, the PRD city groups, the MYR city clusters and the SC urban agglomeration. This is related to car ownership; more than one-half of motor vehicles occur in Chinese megacities. Moreover, this trend will continue as urbanization accelerates in China. Ship emission from the Bohai and East China Seas is also an important mobile source. A similar phenomenon was found in a maritime NO_x emissions study over Chinese seas derived from satellite observations (SI Fig. S16) (Ding et al., 2018). As previously mentioned, it has been estimated that 11.3% of the total NO_x emissions in 2013 came from ships, particularly in the Bohai and East China seas where nine of the top ten cargo throughputs in China's coastal ports are located (Zhang et al., 2016). Regarding microbial processes, edaphic and oceanic sources (especially in marine sediments and estuaries) are important components. Thus, a cultivated region where a large amount of nitrogen fertilizer is consumed is the major source region. This is similar to the source region of biomass burning; the area mainly includes the North China Plain and Sichuan Basin. In addition, the South China Sea (around the Pearl River estuary), East China Sea (around Yangtze River estuary), Korea and Southeast Asian countries are also important source areas. Particularly during summer, warm southeast winds become important drivers of microbial contributions, which was consistent with the peak of this source during summer. There are, of course, reasons for the high temperature and abundant rain that contribute to the high soil emissions.

3.5. Source signals of $PM_{2.5}$ during the heavy pollution stage

In HP stage, $PM_{2.5}$ concentrations were 283 ± 57.9 μg m^{-3}, 158 ± 36.6 μg m^{-3}, 117 ± 14.6 μg m^{-3}, 216 ± 25.6 μg m^{-3} and 257 ± 43.3 μg m^{-3} in Beijing, Shanghai, Guangzhou, Wuhan and Chengdu, respectively, which were all much higher than those for NHP stage (91.8 ± 11.9 μg m^{-3}; 40.9 ± 8.12 μg m^{-3}; 45.5 ± 8.07 μg m^{-3}; 73.8 ± 16.4 μg m^{-3}; 88.2 ± 20.9 μg m^{-3}). Statistically, the HP stage mainly occurred during winter in all five cites. Using linear regression method (SI Table S6), $PM_{2.5}$ concentrations were more related with NO_3^- concentrations ($p < 0.05$) in HP stage, performing as that r values were higher than 0.5. In addition, $NO_3^-/PM_{2.5}$ ratio was significantly (SI Fig. S17; $p < 0.05$) higher during HP stage (11.4%–23.4%) than that during NHP stage (4.99%–10.4%). These evidences were implying that NO_3^- was a vital component for the formation of the heavy $PM_{2.5}$ pollution.

During HP stage, $\delta^{15}N\text{-}NO_3^-$ values were statistically higher than those during NHP stage as shown in SI Fig. S18 ($p < 0.01$). Among the sources considered in the present study, the $\delta^{15}N\text{-}NO_x$ value of coal combustion was the highest (SI Table S4). Thus, the higher $\delta^{15}N\text{-}NO_3^-$ values during HP stage suggested an increased contribution of coal combustion, which was further confirmed by the simulation of Bayesian model (Fig. 5). In addition, SI Fig. S19 displays the geographical pattern of HP stage $PM_{2.5}$ derived from the PSCF modelling. The dominant

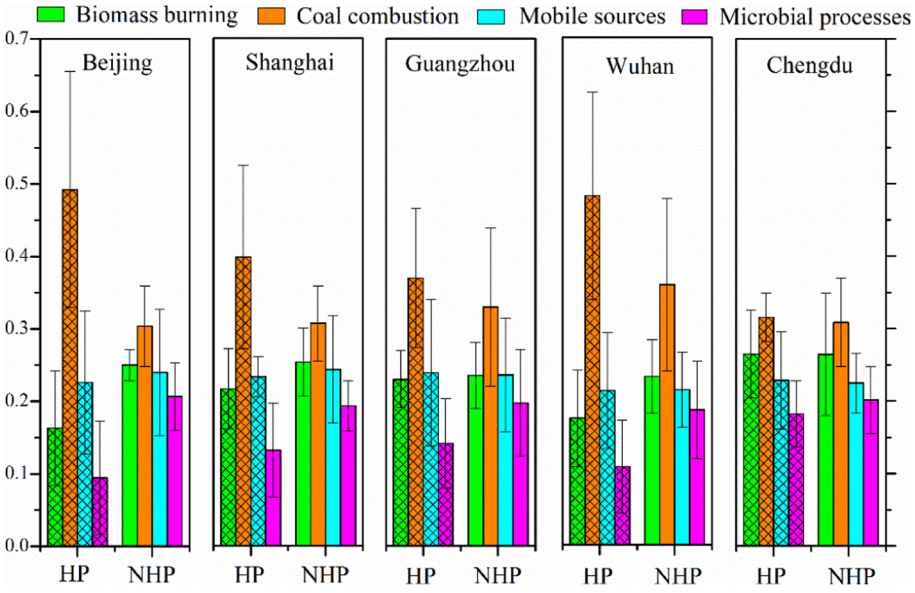

Fig. 5. Contributions of biomass burning, coal combustion, mobile sources and microbial processes to NO_x in HP stage and NHP stage, respectively.

sources were mainly apportioned in North China, similar to that of the coal combustion source for NO_x (Fig. 4). As mentioned above, HP stage basically occurred during winter. Except for the meteorological conditions [e.g. atmospheric boundary layer (Hollaway et al., 2019)], this reflected the key role of residential coal combustion for heating as industrial coal is consumed year round. Based on the characteristics discussed of NO_x, we can infer that coal combustion originating from residential use was the primary source for the heavy $PM_{2.5}$ pollution in Chinese megacities.

4. Conclusion

This study was carried out using $\delta^{15}N\text{-}NO_3^-$, $\delta^{18}O\text{-}NO_3^-$ and dual modelling to investigate the sources, conversion and geographical origin of NO_x in five Chinese megacities. Important findings of this study include i). $\delta^{15}N\text{-}NO_3^-$ and $\delta^{18}O\text{-}NO_3^-$ both had a rising tendency as ambient temperature drops, attributing largely to the NO_x source change. ii). The proportion for the ·OH pathway of NO_x conversion had a clear seasonal variation with higher value in summer and lower value in winter, which also shared significant correlation with latitude all year-round ($p < 0.01$). iii). Coal combustion was the most important source of NO_x at the five megacities, which, geographically, was derived from North China and other south-central developed regions. Apart from Chengdu, mobile sources was the second largest contributor to NO_x. It was extensive, but rather uniformly distributed all around the typical urban agglomerations. Biomass burning and microbial processes shared similar source areas, mostly originating from the North China Plain and Sichuan Basin. iv). Residential coal combustion was the primary source of heavy $PM_{2.5}$ pollution in the five megacities. It is undeniable that the apportionment results from 2013 to 2014 may have a certain lag effect on the current NO_x treatment. However, this period was exactly the starting point of large-scale pollution control in China [e.g. Action Plan for Air Pollution Prevention and Control (2013–17)], so our study can provide a background reference (including sources, conversion and geographical origin) for the implementation effect of NO_x controls. For example, we find that residential coal combustion was the main source of NO_x, and Chinese government happened to extensively promote the project of changing fuel from coal to natural gas from 2014, which has been widely questioned by now (e.g. The General Department of the National Energy Administration issued a letter asking for opinions of this project on July 3, 2019). Therefore, our isotopic footprint is very instructive for related researches in the future. We believe that this source apportionment of NO_x will inevitably provide an important indicator for the air pollution control in China.

5. Data availability

Data are available from the corresponding author on request.

CRediT authorship contribution statement

Zheng Zong: Data curation, Methodology, Software, Visualization, Investigation, Writing - original draft, Writing - review & editing. **Yang Tan:** Investigation, Methodology. **Xiao Wang:** Investigation, Methodology, Visualization. **Chongguo Tian:** Conceptualization, Methodology, Software, Supervision, Validation, Writing - review & editing. **Jun Li:** Conceptualization, Methodology, Software, Supervision, Validation, Writing - review & editing. **Yunting Fang:** Methodology, Software, Supervision, Validation. **Yingjun Chen:** Methodology, Software, Supervision, Validation. **Song Cui:** Visualization, Investigation. **Gan Zhang:** Methodology, Software, Supervision, Validation.

Declaration of Competing Interest

The authors declare that they have no known competing financial interests or personal relationships that could have appeared to influence the work reported in this paper.

Acknowledgement

This research was financially supported by Project funded by China Postdoctoral Science Foundation (2017LH020; 2017M622815), the Natural Scientific Foundation of China (NSFC; Grant Nos: 41977190 and 41907198), Guangdong Foundation for Program of Science and Technology Research (Grant No. 2017B030314057). The authors gratefully acknowledge the National Oceanic and Atmospheric Administration's Air Resources Laboratory for providing the HYSPLIT transport model.

Appendix A. Supplementary material

Supplementary data to this article can be found online at https://doi.org/10.1016/j.envint.2020.105592.

References

Alexander, B., Hastings, M.G., Allman, D.J., Dachs, J., Thornton, J.A., Kunasek, S.A., 2009. Quantifying atmospheric nitrate formation pathways based on a global model of the oxygen isotopic composition ($\Delta^{17}O$) of atmospheric nitrate. Atmos. Chem. Phys. 9, 5043–5056. https://doi.org/10.5194/acp-9-5043-2009.

Bressi, M., Sciare, J., Ghersi, V., Mihalopoulos, N., Petit, J.E., Nicolas, J.B., Moukhtar, S., Rosso, A., Féron, A., Bonnaire, N., Poulakis, E., Theodosi, C., 2014. Sources and geographical origins of fine aerosols in Paris (France). Atmos. Chem. Phys. 14, 8813–8839. https://doi.org/10.5194/acp-14-8813-2014.

Cai, S., Li, Q., Wang, S., Chen, J., Ding, D., Zhao, B., Yang, D., Hao, J., 2018. Pollutant emissions from residential combustion and reduction strategies estimated via a village-based emission inventory in Beijing. Environ. Pollut. 238, 230–237. https://doi.org/10.1016/j.envpol.2018.03.036.

Chang, Y., Zhang, Y., Tian, C., Zhang, S., Ma, X., Cao, F., Liu, X., Zhang, W., Kuhn, T., Lehmann, M.F., 2018. Nitrogen isotope fractionation during gas-to-particle conversion of NO_x to NO_3^- in the atmosphere – implications for isotope-based NO_x source apportionment. Atmos. Chem. Phys. 18, 11647–11661. https://doi.org/10.5194/acp-18-11647-2018.

Chen, S., Xu, L., Zhang, Y., Chen, B., Wang, X., Zhang, X., Zheng, M., Chen, J., Wang, W., Sun, Y., Fu, P., Wang, Z., Li, W., 2017. Direct observations of organic aerosols in common wintertime hazes in North China: insights into direct emissions from Chinese residential stoves. Atmos. Chem. Phys. 17, 1259–1270. https://doi.org/10.5194/acp-17-1259-2017.

Ding, A.J., Huang, X., Nie, W., Sun, J.N., Kerminen, V.M., Petäjä, T., Su, H., Cheng, Y.F., Yang, X.Q., Wang, M.H., Chi, X.G., Wang, J.P., Virkkula, A., Guo, W.D., Yuan, J., Wang, S.Y., Zhang, R.J., Wu, Y.F., Song, Y., Zhu, T., Zilitinkevich, S., Kulmala, M., Fu, C.B., 2016. Enhanced haze pollution by black carbon in megacities in China. Geophys. Res. Lett. 43, 2873–2879. https://doi.org/10.1002/2016gl067745.

Ding, J., van der, A.R.J., Mijling, B., Jalkanen, J.P., Johansson, L., Levelt, P.F., 2018. Maritime NO_x emissions over chinese seas derived from satellite observations. Geophys. Res. Lett. 45, 2031–2037. https://doi.org/10.1002/2017gl076788.

Elliott, E.M., Kendall, C., Boyer, E.W., Burns, D.A., Lear, G.G., Golden, H.E., Harlin, K., Bytnerowicz, A., Butler, T.J., Glatz, R., 2009. Dual nitrate isotopes in dry deposition: Utility for partitioning NO_x source contributions to landscape nitrogen deposition. J. Geophys. Res.-Biogeo. 114. https://doi.org/10.1029/2008jg000889.

Elliott, E.M., Yu, Z., Cole, A.S., Coughlin, J.G., 2019. Isotopic advances in understanding reactive nitrogen deposition and atmospheric processing. Sci. Total Environ. 662, 393–403. https://doi.org/10.1016/j.scitotenv.2018.12.177.

Fang, Y.T., Koba, K., Wang, X.M., Wen, D.Z., Li, J., Takebayashi, Y., Liu, X.Y., Yoh, M., 2011. Anthropogenic imprints on nitrogen and oxygen isotopic composition of precipitation nitrate in a nitrogen-polluted city in southern China. Atmos. Chem. Phys. 11, 1313–1325. https://doi.org/10.5194/acp-11-1313-2011.

Felix, J.D., Elliott, E.M., Shaw, S.L., 2012. Nitrogen isotopic composition of coal-fired power plant NO_x: influence of emission controls and implications for global emission inventories. Environ. Sci. Technol. 46, 3528–3535. https://doi.org/10.1021/es203355v.

Felix, J.D., Elliott, E.M., 2014. Isotopic composition of passively collected nitrogen dioxide emissions: Vehicle, soil and livestock source signatures. Atmos. Environ. 92, 359–366. https://doi.org/10.1016/j.atmosenv.2014.04.005.

Gao, R., Jiang, W., Gao, W., Sun, S., 2017. Emission inventory of crop residue open burning and its high-resolution spatial distribution in 2014 for Shandong province, China. Atmos. Pollut. Res. 8, 545–554. https://doi.org/10.1016/j.apr.2016.12.009.

Guo, S., Hu, M., Zamora, M.L., Peng, J., Shang, D., Zheng, J., Du, Z., Wu, Z., Shao, M., Zeng, L., Molina, M.J., Zhang, R., 2014. Elucidating severe urban haze formation in China. P. Natl. Acad. Sci. U. S. A. 111, 17373–17378. https://doi.org/10.1073/pnas.1419604111.

Hastings, M.G., Jarvis, J.C., Steig, E.J., 2009. Anthropogenic impacts on nitrogen isotopes of ice-core nitrate. Science 324, 1288. https://doi.org/10.1126/science.1170510.

He, P., Xie, Z., Chi, X., Yu, X., Fan, S., Kang, H., Liu, C., Zhan, H., 2018. Atmospheric $\Delta^{17}O$ (NO_3^-) reveals nocturnal chemistry dominates nitrate production in Beijing haze. Atmos. Chem. Phys. 18, 14465–14476. https://doi.org/10.5194/acp-18-14465-2018.

Hollaway, M., Wild, O., Yang, T., Sun, Y., Xu, W., Xie, C., Whalley, L., Slater, E., Heard, D., Liu, D., 2019. Photochemical impacts of haze pollution in an urban environment. Atmos. Chem. Phys. 19, 9699–9714. https://doi.org/10.5194/acp-19-9699-2019.

Jaeglé, L., Martin, R.V., Chance, K., Steinberger, L., Kurosu, T.P., Jacob, D.J., Modi, A.I., Yoboué, V., Sigha-Nkamdjou, L., Galy-Lacaux, C., 2004. Satellite mapping of rain-induced nitric oxide emissions from soils. J. Geophys. Res. - Atmos. 109. https://doi.org/10.1029/2004jd004787.

Jeong, U., Kim, J., Lee, H., Jung, J., Kim, Y.J., Song, C.H., Koo, J.-H., 2011. Estimation of the contributions of long range transported aerosol in East Asia to carbonaceous aerosol and PM concentrations in Seoul, Korea using highly time resolved measurements: a PSCF model approach. J. Environ. Monitor. 13, 1905–1918. https://doi.org/10.1039/c0em00659a.

Kharol, S.K., Martin, R.V., Philip, S., Vogel, S., Henze, D.K., Chen, D., Wang, Y., Zhang, Q., Heald, C.L., 2013. Persistent sensitivity of Asian aerosol to emissions of nitrogen oxides. Geophys. Res. Lett. 40, 1021–1026. https://doi.org/10.1002/grl.50234.

Li, C., Borken-Kleefeld, J., Zheng, J., Yuan, Z., Ou, J., Li, Y., Wang, Y., Xu, Y., 2018a. Decadal evolution of ship emissions in China from 2004 to 2013 by using an integrated AIS-based approach and projection to 2040. Atmos. Chem. Phys. 18, 6075–6093. https://doi.org/10.5194/acp-18-6075-2018.

Li, H., Zhang, Q., Zheng, B., Chen, C., Wu, N., Guo, H., Zhang, Y., Zheng, Y., Li, X., He, K., 2018b. Nitrate-driven urban haze pollution during summertime over the North China Plain. Atmos. Chem. Phys. 18, 5293–5306. https://doi.org/10.5194/acp-18-5293-2018.

Li, J., Li, Y., Bo, Y., Xie, S., 2016. High-resolution historical emission inventories of crop residue burning in fields in China for the period 1990–2013. Atmos. Environ. 138, 152–161. https://doi.org/10.1016/j.atmosenv.2016.05.002.

Liu, D., Lin, T., Shen, K., Li, J., Yu, Z., Zhang, G., 2016. Occurrence and concentrations of halogenated flame retardants in the atmospheric fine particles in Chinese cities. Environ. Sci. Technol. 50, 9846–9854. https://doi.org/10.1021/acs.est.6b01685.

Liu, J., Li, J., Zhang, Y., Liu, D., Ding, P., Shen, C., Shen, K., He, Q., Ding, X., Wang, X., Chen, D., Szidat, S., Zhang, G., 2014. Source apportionment using radiocarbon and organic tracers for $PM_{2.5}$ carbonaceous aerosols in Guangzhou, South China: contrasting local- and regional-scale haze events. Environ. Sci. Technol. 48, 12002–12011. https://doi.org/10.1021/es503102w.

Luo, L., Wu, Y., Xiao, H., Zhang, R., Lin, H., Zhang, X., Kao, S.J., 2019. Origins of aerosol nitrate in Beijing during late winter through spring. Sci. Total Environ. 653, 776–782. https://doi.org/10.1016/j.scitotenv.2018.10.306.

Madaniyazi, L., Nagashima, T., Guo, Y., Pan, X., Tong, S., 2016. Projecting ozone-related mortality in East China. Environ. Int. 92–93, 165–172. https://doi.org/10.1016/j.envint.2016.03.040.

McIlvin, M.R., Altabet, M.A., 2005. Chemical conversion of nitrate and nitrite to nitrous oxide for nitrogen and oxygen isotopic analysis in freshwater and seawater. Anal. Chem. 77, 5589–5595. https://doi.org/10.1021/ac050528s.

Ming, Z., Xiaohu, Z., Ping, Z., Jun, D., 2016. Overall review of China's thermal power development with emphatic analysis on thermal powers' cost and benefit. Renew. Sust. Energ. Rev. 63, 152–157. https://doi.org/10.1016/j.rser.2016.05.057.

Moore, J.W., Semmens, B.X., 2008. Incorporating uncertainty and prior information into stable isotope mixing models. Ecol. Lett. 11, 470–480. https://doi.org/10.1111/j.1461-0248.2008.01163.x.

Morin, S., Savarino, J., Frey, M.M., Yan, N., Bekki, S., Bottenheim, J.W., Martins, J.M.F., 2008. Tracing the origin and fate of NO_x in the arctic atmosphere using stable isotopes in nitrate. Science 322, 730–732. https://doi.org/10.1126/science.1161910.

Morin, S., Savarino, J., Frey, M.M., Domine, F., Jacobi, H.W., Kaleschke, L., Martins, J.M.F., 2009. Comprehensive isotopic composition of atmospheric nitrate in the Atlantic Ocean boundary layer from 65°S to 79°N. J. Geophys. Res. 114. https://doi.org/10.1029/2008jd010696.

Ning, J., Liu, J., Kuang, W., Xu, X., Zhang, S., Yan, C., Li, R., Wu, S., Hu, Y., Du, G., Chi, W., Pan, T., Ning, J., 2018. Spatiotemporal patterns and characteristics of land-use change in China during 2010–2015. J. Geogr. Sci. 28, 547–562. https://doi.org/10.1007/s11442-018-1490-0.

Pan, Y., Tian, S., Liu, D., Fang, Y., Zhu, X., Zhang, Q., Zheng, B., Michalski, G., Wang, Y., 2016. Fossil fuel combustion-related emissions dominate atmospheric ammonia sources during severe haze episodes: evidence from $\delta^{15}N$-stable isotope in size-resolved aerosol ammonium. Environ. Sci. Technol. 50, 8049–8056. https://doi.org/10.1021/acs.est.6b00634.

Parnell, A.C., Phillips, D.L., Bearhop, S., Semmens, B.X., Ward, E.J., Moore, J.W., Jackson, A.L., Grey, J., Kelly, D.J., Inger, R., 2013. Bayesian stable isotope mixing models. Environmetrics 24, 387–399. https://doi.org/10.1002/env.2221.

Qiu, X., Duan, L., Chai, F., Wang, S., Yu, Q., Wang, S., 2016. Deriving high-resolution emission inventory of open biomass burning in china based on satellite observations. Environ. Sci. Technol. 50, 11779–11786. https://doi.org/10.1021/acs.est.6b02705.

Si, Y., Wang, H., Cai, K., Chen, L., Zhou, Z., Li, S., 2019. Long-term (2006–2015) variations and relations of multiple atmospheric pollutants based on multi-remote sensing data over the North China Plain. 113323–113323. Environ. Pollut. (Barking, Essex 1987) 255. https://doi.org/10.1016/j.envpol.2019.113323.

Song, W., Wang, Y.L., Yang, W., Sun, X.C., Tong, Y.D., Wang, X.M., Liu, C.Q., Bai, Z.P., Liu, X.Y., 2019. Isotopic evaluation on relative contributions of major NO_x sources to nitrate of $PM_{2.5}$ in Beijing. Environ. Pollut. 248, 183–190. https://doi.org/10.1016/j.envpol.2019.01.081.

Spivakovsky, C.M., Logan, J.A., Montzka, S.A., Balkanski, Y.J., Foreman-Fowler, M., Jones, D.B.A., Horowitz, L.W., Fusco, A.C., Brenninkmeijer, C.A.M., Prather, M.J., Wofsy, S.C., McElroy, M.B., 2000. Three-dimensional climatological distribution of tropospheric OH: Update and evaluation. J. Geophys. Res.-Atmos. 105, 8931–8980. https://doi.org/10.1029/1999jd901006.

Sun, Y., Jiang, Q., Wang, Z., Fu, P., Li, J., Yang, T., Yin, Y., 2014. Investigation of the sources and evolution processes of severe haze pollution in Beijing in January 2013. J. Geophys. Res.-Atmos. 119, 4380–4398. https://doi.org/10.1002/2014jd021641.

Tao, J., Gao, J., Zhang, L., Zhang, R., Che, H., Zhang, Z., Lin, Z., Jing, J., Cao, J., Hsu, S., 2014. C.: $PM_{2.5}$ pollution in a megacity of southwest China: source apportionment and implication. Atmos. Chem. Phys. 14, 8679–8699. https://doi.org/10.5194/acp-14-8679-2014.

Tong, D., Zhang, Q., Liu, F., Geng, G., Zheng, Y., Xue, T., Hong, C., Wu, R., Qin, Y., Zhao, H., Yan, L., He, K., 2010. Current emissions and future mitigation pathways of coal-fired power plants in China from to 2030. Environ. Sci. Technol. 2018. https://doi.org/10.1021/acs.est.8b02919.

Vicars, W.C., Bhattacharya, S.K., Erbland, J., Savarino, J., 2012. Measurement of the ^{17}O-excess ($\Delta^{17}O$) of tropospheric ozone using a nitrite-coated filter. Rapid Commun. Mass Sp. 26, 1219–1231. https://doi.org/10.1002/rcm.6218.

Walters, W.W., Michalski, G., 2015. Theoretical calculation of nitrogen isotope equilibrium exchange fractionation factors for various NO_y molecules. Geochim. Cosmochim. Ac. 164, 284–297. https://doi.org/10.1016/j.gca.2015.05.029.

Walters, W.W., Tharp, B.D., Fang, H., Kozak, B.J., Michalski, G., 2015. Nitrogen isotope composition of thermally produced NO_x from various fossil-fuel combustion sources. Environ. Sci. Technol. 49, 11363–11371. https://doi.org/10.1021/acs.est.5b02769.

Walters, W.W., Michalski, G., 2016. Theoretical calculation of oxygen equilibrium isotope fractionation factors involving various NO_y molecules, OH, and H_2O and its implications for isotope variations in atmospheric nitrate. Geochim. Cosmochim. Ac. 191, 89–101. https://doi.org/10.1016/j.gca.2016.06.039.

Wang, X., Chen, Y., Tian, C., Huang, G., Fang, Y., Zhang, F., Zong, Z., Li, J., Zhang, G., 2014. Impact of agricultural waste burning in the Shandong Peninsula on carbonaceous aerosols in the Bohai Rim, China. Sci. Total Environ. 481, 311–316. https://doi.org/10.1016/j.scitotenv.2014.02.064.

Wankel, S.D., Kendall, C., Francis, C.A., Paytan, A., 2006. Nitrogen sources and cycling in the San Francisco Bay Estuary: A nitrate dual isotopic composition approach. Limnol. Oceanogr. 51, 1654–1664. https://doi.org/10.4319/lo.2006.51.4.1654.

Wen, L., Xue, L., Wang, X., Xu, C., Chen, T., Yang, L., Wang, T., Zhang, Q., Wang, W., 2018. Summertime fine particulate nitrate pollution in the North China Plain: increasing trends, formation mechanisms and implications for control policy. Atmos. Chem. Phys. 18, 11261–11275. https://doi.org/10.5194/acp-18-11261-2018.

Wu, R., Xie, S., 2018. Spatial distribution of secondary organic aerosol formation potential in china derived from speciated anthropogenic volatile organic compound emissions. Environ. Sci. Technol. 52, 8146–8156. https://doi.org/10.1021/acs.est.8b01269.

Xie, Y., Wang, Y., Zhang, K., Dong, W., Lv, B., Bai, Y., 2015. Daily estimation of ground-level $PM_{2.5}$ concentrations over beijing using 3 km resolution MODIS AOD. Environ. Sci. Technol. 49, 12280–12288. https://doi.org/10.1021/acs.est.5b01413.

Xu, D., Zhang, Y., Zhou, L., Li, T., 2018. Acute effects of $PM_{2.5}$ on lung function parameters in schoolchildren in Nanjing, China: a panel study. Environ. Sci. Pollu. Res. 25, 14989–14995. https://doi.org/10.1007/s11356-018-1693-z.

Xu, W., Sun, Y., Wang, Q., Zhao, J., Wang, J., Ge, X., Xie, C., Zhou, W., Du, W., Li, J., Fu, P., Wang, Z., Worsnop, D.R., Coe, H., 2019. Changes in aerosol chemistry From 2014 to 2016 in winter in Beijing: insights from high-resolution aerosol mass spectrometry. J. Geophys. Res.-Atmos. 124, 1132–1147. https://doi.org/10.1029/2018jd029245.

Yearbook CES. Part III: production statistic; 2014.

Yearbook CS. Part XVI: transport, post, and telecommunication services; 2015.

Yihui, D., Chan, J.C.L., 2005. The East Asian summer monsoon: an overview. Meteorol. Atmos. Phys. 89, 117–142. https://doi.org/10.1007/s00703-005-0125-z.

Zhang, F., Chen, Y., Tian, C., Lou, D., Li, J., Zhang, G., Matthias, V., 2016. Emission factors for gaseous and particulate pollutants from offshore diesel engine vessels in China. Atmos. Chem. Phys. 16, 6319–6334. https://doi.org/10.5194/acp-16-6319-2016.

Zhang, Y.L., Li, J., Zhang, G., Zotter, P., Huang, R.J., Tang, J.H., Wacker, L., Prevot, A.S., Szidat, S., 2014. Radiocarbon-based source apportionment of carbonaceous aerosols at a regional background site on Hainan Island, South China. Environ. Sci. Technol. 48, 2651–2659. https://doi.org/10.1021/es4050852.

Zhang, Y.L., Cao, F., 2015. Fine particulate matter (PM2.5) in China at a city level. Sci. Rep. 5 (14884). https://doi.org/10.1038/srep14884.

Zhao, P.S., Dong, F., He, D., Zhao, X.J., Zhang, X.L., Zhang, W.Z., Yao, Q., Liu, H.Y., 2013. Characteristics of concentrations and chemical compositions for $PM_{2.5}$ in the region of Beijing, Tianjin, and Hebei, China. Atmos. Chem. Phys. 13, 4631–4644. https://doi.org/10.5194/acp-13-4631-2013.

Zong, Z., Chen, Y., Tian, C., Fang, Y., Wang, X., Huang, G., Zhang, F., Li, J., Zhang, G., 2015. Radiocarbon-based impact assessment of open biomass burning on regional carbonaceous aerosols in North China. Sci. Total Environ. 518–519, 1–7. https://doi.org/10.1016/j.scitotenv.2015.01.113.

Zong, Z., Wang, X., Tian, C., Chen, Y., Qu, L., Ji, L., Zhi, G., Li, J., Zhang, G., 2016. Source apportionment of $PM_{2.5}$ at a regional background site in North China using PMF linked with radiocarbon analysis: insight into the contribution of biomass burning. Atmos. Chem. Phys. 16, 11249–11265. https://doi.org/10.5194/acp-16-11249-2016.

Zong, Z., Wang, X., Tian, C., Chen, Y., Fang, Y., Zhang, F., Li, C., Sun, J., Li, J., Zhang, G., 2017. First assessment of NO_x sources at a regional background site in North China using isotopic analysis linked with modeling. Environ. Sci. Technol. 51, 5923–5931. https://doi.org/10.1021/acs.est.6b06316.